SUPPORTING INFORMATION

Synthesis by Thermal Decomposition of Two Iron Hydroxyfluorides: Structural Effects of Li insertion

Kévin Lemoine,[†] Leiting Zhang,[‡] Damien Dambournet,[§ #] Jean-Marc Grenèche,[†] Annie Hémon-Ribaud,[†] Marc Leblanc,[†] Olaf J. Borkiewicz,[⊥] Jean-Marie Tarascon,[# ‡] Vincent Maisonneuve,[†] Jérôme Lhoste[* †]

[†] Institut des Molécules et des Matériaux du Mans (IMMM) - UMR 6283 CNRS, Le Mans Université, Avenue Olivier Messiaen, 72085 Le Mans Cedex 9, France

[‡] Collège de France, Chaire de Chimie du Solide et de l'Energie, UMR 8260, 11 Place Marcelin Berthelot, 75231 Paris Cedex 5, France

[§] Sorbonne Universités, Physico-chimie des électrolytes et nano-systèmes interfaciaux, PHENIX, 75005 Paris, France

[#] Réseau sur le Stockage Electrochimique de l'Energie (RS2E), FR CNRS 3459, 80039 Amiens, France

[⊥] X-ray Science Division, Advanced Photon Source, Argonne National Laboratory, Argonne, Illinois 60439, United States

Table S1. Crystal data* and structure of $Fe_3F_8(H_2O)_2$ and $Fe_2F_5(H_2O)_2$ and refinement parameters obtained from powder XRD.

Compounds	**$Fe_3F_8(H_2O)_2$**		**$Fe_2F_5(H_2O)_2$**	
Data	Crystal	Powder	Crystal	Powder
Molecular weight (g mol^{-1})	355.58		242.73	
Crystal system	Monoclinic		Orthorhombic	
Space group	*C*2/*m*		*Imma*	
a (Å)	7.586(2)	7.588(1)	7.485(1)	7.482(1)
b (Å)	7.472(2)	7.472(1)	10.888(1)	10.887(1)
c (Å)	7.432(2)	7.463(1)	6.663(1)	6.665(1)
β (°)	118.230(4)	118.70(1)	-	-
V ($Å^3$),	371.1(2)	371.16(1)	542.98(5)	542.91(2)
Z, $\rho_{calc.}$ (g cm^{-3})	2, 3.182	2, 3.182	4, 2.969	4, 2.970
Wavelength (Å)	MoK_α	CoK_α	MoK_α	CoK_α
μ/mm-1	5.900	-	5.381	
2θ range (°)	8.1 – 56.4	10 – 130	7.2 – 60.0	10 – 130
Limiting indices	$-10 \le h \le 10$ $-9 \le k \le 9$ $-9 \le l \le 9$	- - -	$-6 \le h \le 10$ $-15 \le k \le 9$ $-9 \le l \le 9$	- - -
Collected reflections	2387	-	1755	-
Refl. uni.	480	494	446	359
Refined parameters	41	64	32	57
Goodness-of-fit on F^2	1.167	-	1.104	-
Final R indices [I>2σ(I)]	$R_1 = 0.0222$ $Rw_1 = 0.0617$	- -	$R_1 = 0{,}0266$ $Rw_1 = 0.0538$	- -
R indices (all data)	$R_1 = 0.0221$ $Rw_1 = 0.0617$	- -	$R_1 = 0{,}0223$ $Rw_1 = 0.0508$	- -
R_p/R_{wp}	-	0.110/0.085	-	0.200/0.168
R_B/R_f	-	0.042/0.037	-	0.101/0.125
Largest diff. peak and hole/e.$Å^{-3}$	0.453/-1.109	-	0.360/-0.539	

$Fe_3F_8(H_2O)_2$, ISCD-38366, monoclinic *C*2/*m*, a = 7.609(5) Å, b = 7.514(6) Å, c = 7.453(4) Å, β= 118.21(3)°, V = 375.50 A^3
$Fe_2F_5(H_2O)_2$, ISCD-201737, orthorhombic *Imma*, a = 7.477(1) Å, b = 10.862(2), c = 6.652(1) Å, V = 540.24 A^3

*Crystals were selected under polarizing optical microscope and mounted on MicroMount needles (MiTiGen) for single-crystal X-ray diffraction experiments. X-ray intensity data were collected on a Bruker APEX II Quazar diffractometer (4 circle Kappa goniometer, CCD detector) using Iμs microfocus source (Mo-K_α radiation with λ = 0.71073 Å) at 296 K. The structure solutions were obtained by direct methods, developed by successive difference Fourier

syntheses, and refined by full-matrix least-squares on all F^2 data using SHELX program suite in Bruker APEX2 interface.

Table S2. Atomic coordinates and equivalent ADP of $Fe_2F_5(H_2O)_2$ (**crystal** and *powder* data).

Atom	Site	x	y	z	B_{eq} (Å^2)
Fe^{2+}(1)	4a	**0** *0*	**0** *0*	**0** *0*	**0.80(1)** 2.2(1)
Fe^{3+}(2)	4c	**¼** *¼*	**¼** *¼*	**¼** *¼*	**0.59(2)** 2.1(1)
O(1)	8h	**½** *½*	**0.5676(3)** *0.5618(4)*	**0.2033(3)** *0.2027(6)*	**1.97(5)** 3.5(1)
H(1)	16j	**0.4020(7)** *0.4020*	**0.588(2)** *0.588*	**0.133(2)** *0.133*	**2.38** 5.0
F(1)	16j	**0.2019(2)** *0.1980(4)*	**0.1253(2)** *0.1232(3)*	**0.0541(2)** *0.0606(4)*	**1.38(3)** 3.5(1)
F(2)	4e	**0** *0*	**¼** *¼*	**0.3344(4)** *0.3120(8)*	**1.18(4)** 3.5(1)

Table S3. Atomic coordinates and equivalent ADP of $Fe_3F_8(H_2O)_2$ (**crystal** and *powder* data).

Atom	Site	x	y	z	B_{eq} (Å^2)
Fe^{2+}(1)	2b	**0** *0*	**½** *½*	**0** *0*	**0.77(2)** *1.37(7)*
Fe^{3+}(2)	4f	**¼** *¼*	**¼** *¼*	**½** *½*	**0.49(1)** *1.82(5)*
O(1)	4i	**0.2450(5)** *0.2444(4)*	**0** *0*	**0.0423(5)** *0.0324(5)*	**2.06(6)** *2.40(5)*
H(1)	8j	**0.214(7)** *0.214*	**0.097(6)** *0.97*	**0.086(7)** *-0.086*	**4.0(9)** *5.0*
F(1)	4h	**0** *0*	**0.2952(3)** *0.2962(3)*	**½** *½*	**1.45(4)** *2.40(5)*
F(2)	4i	**0.1809(3)** *0.1798(4)*	**0** *0*	**0.4384(3)** *0.4412(5)*	**1.13(4)** *2.40(5)*
F(3)	8j	**0.1294(2)** *0.1272(3)*	**0.2975(2)** *0.3018(3)*	**0.2141(2)** *0.2171 (2)*	**1.41(3)** *2.40(5)*

Figure S1. Thermogravimetric under ambient of $Fe_{2.5}F_{0.25}(OH)_{0.25}$

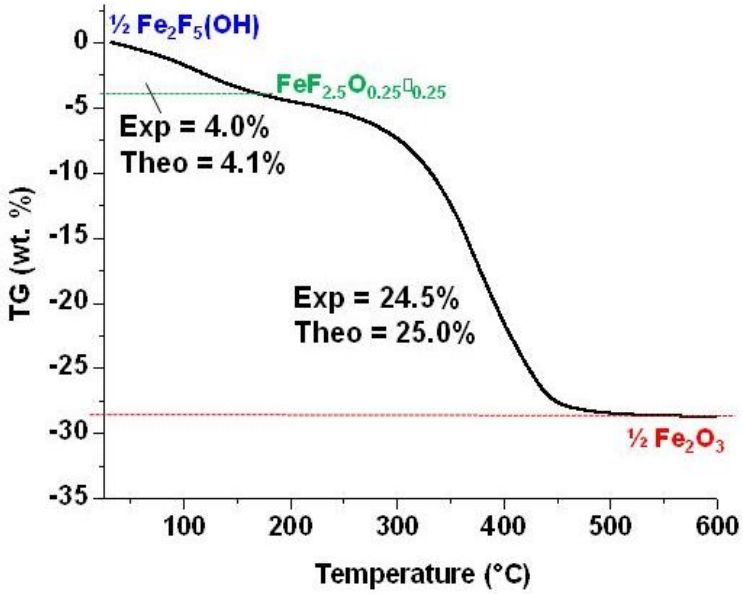

Figure S2. Thermogravimetric (TGA-MS) curve and ionic curves m/z (= +17, +18, +19) performed under N_2 of $Fe_3F_8(H_2O)_2$

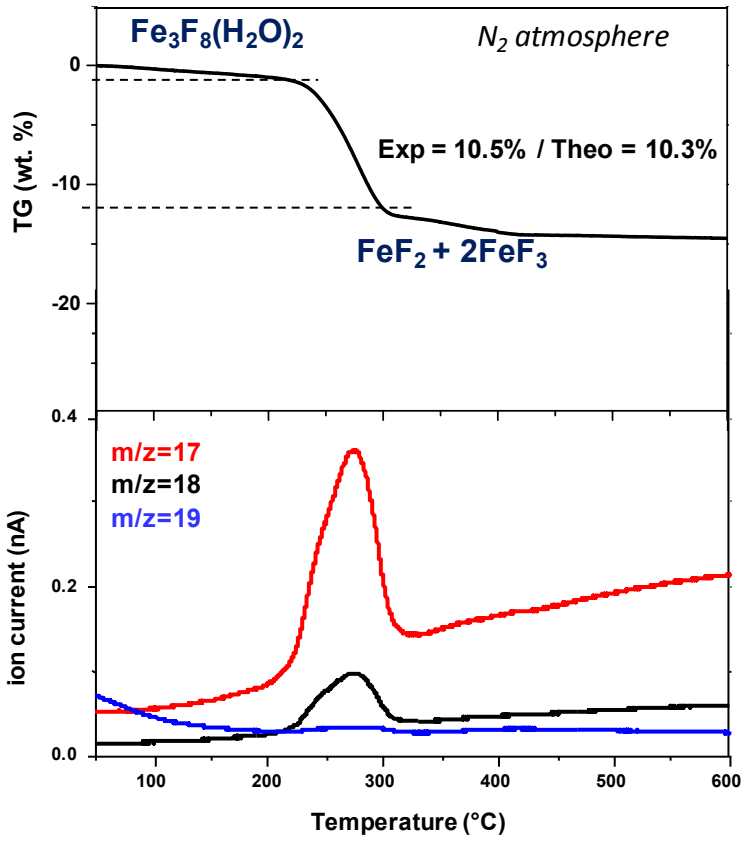

Table S4. Crystallographic data of $FeF_{2.5}(OH)_{0.5}$ based on the different structural models.

Structural model	**$FeF_{2.5}(OH)_{0.5}$**	**$FeF_{2.5}(OH)_{0.5}\cdot 0.5H_2O$**
Crystal system	Cubic	
Space group	*Fd*-3*m*	
a (Å)	10.3438(8)	10.3563(5)
V (Å^3), Z	1106.7(2), 16	1110.7(1), 16
Wavelength (Å)	CoK_α	
$\rho_{calc.}$ (g cm^{-3})	2.673	2.855
2θ range (°)	10-140	
Refl. uni.	100	100
Refined parameters	54	55
R_p/R_{wp}	0.283/0.238	0.167/0.133
R_B/R_f	0.121/0.074	0.064/0.048
χ^2	48.3	15.1

Table S5. ^{57}Fe Mössbauer Hyperfine Parameters from litterature

Temperature		Fe^{n+}	δ	$\Delta E_Q/2\varepsilon$	B_{hf}	%
Pyrochlore FeF_3 (Y.Calage *et al.*, J. Solid State Chem.[1])						
300 K	1 doublet	Fe^{3+}	0.48	0.24	-	
HTB $FeF_3{\cdot}0.33H_2O$ (Y.Calage *et al.*, J. Magn. Magn. Mater.[2])						
300 K	1 doublet	Fe^{3+}	0.44	0.64	-	
77 K	1 sextuplet	Fe^{3+}	0.54	-0.12	51	
HTB $FeF_3{\cdot}0.33H_2O$ (M. Leblanc *et al.*, J. Solid State Chem.[3])						
300 K	1 doublet	Fe^{3+}	0.44	0.64	-	
77 K	1 sextuplet	Fe^{3+}	0.54	-0.12	51	
HTB $FeF_3{\cdot}0.33H_2O$ (Y. Guo *et al.*, ChemCatChem[4])						
300 K	1 doublet	Fe^{3+}	0.44	0.61	-	
HTB FeF_3 (N. Louvain *et al.*, CrystEngComm[5])						
300 K	1 doublet	Fe^{3+}	0.46	0.17	-	50
	1 sextuplet	Fe^{3+}(r-FeF_3)	0.49	-0.07	37	50
HTB $FeF_{2.2}(OH)_{0.8}{\cdot}0.33H_2O$ (M. Duttine *et al.*, Chem. Mat.[6])						
300 K	1 doublet	Fe^{3+}	0.44	0.61	-	
HTB $FeF_{2.2}O_{0.4}\square_{0.4}$ (M. Duttine *et al.*, Chem. Mat.[6])						
300 K	3 doublets	Fe^{3+}	0.45	0.17	-	52
			0.40	0.64	-	33
			0.35	1.19	-	15
HTB $FeF_{2.2}(OH)_{0.8}{\cdot}0.33H_2O$ under F_2 (M. Duttine *et al.*, Chem. Mat.[6])						
300 K	1 doublet	Fe^{3+}	0.48	0.19	-	
HTB FeF_3 (A. Pohl *et al.*, J. Power Sources[7])						
300K	3 doublets	Fe^{3+}	0.47	0.54	-	62
		Fe^{3+}	0.50	0.22	-	28
		Fe^{2+} (FeF_2)	1.14	2.56	-	7
	1 sextuplet	Fe^{3+}(r-FeF_3)	0.46	0.01	40	3
HTB FeF_3 (Thesis D. Delbegue, 2017)						
300 K	1 doublet	Fe^{3+}	0.47	0.20	-	

Table S6. Crystallographic data of HTB structure based on different structural models.

Structural model	**$FeF_{2.66}(OH)_{0.34}\cdot 0.13H_2O$**	**$FeF_{2.66}(OH)_{0.34}\cdot 0.21H_2O$**
Crystal system	Orthorhombic	Hexagonal
Space group	*Cmcm*	P$6_3/m$
a (Å)	7.396(1)	7.396(1)
b (Å)	12.807(1)	-
c (Å)	7.545(1)	7.545(1)
V (Å^3), Z	714.7(1),12	357.4(1), 6
Wavelength (Å)	CoK_α	
$\rho_{calc.}$ (g cm^{-3})	3.177	3.214
2θ range (°)	10-140	
Refl. uni.	565	346
Refined parameters	58	55
R_p/R_{wp}	0.217/0.124	0.223/0.128
R_B/R_f	0.055/0.072	0.068/0.074
χ^2	3.57	3.81

Table S7. Atomic coordinates and equivalent ADP of $FeF_{2.66}(OH)_{0.34}\cdot 0.13H_2O$ with the *Cmcm* space group.

Atom	**Site**	**x**	**y**	**z**
Fe^{3+}(1)	4b	**0**	**½**	**0**
Fe^{3+}(2)	8d	**¼**	**¼**	**0**
F(1)	8f	**0**	**0.1638(6)**	**0.5469(16)**
O(1)	8f	**0**	**0.1638(6)**	**0.5469(16)**
F(2)	4h	**0.1715(9)**	**0.3900(8)**	**0.0235(12)**
F(3)	4i	**0**	**0.5274(15)**	**¼**
F(4)	8j	**0.206(2)**	**0.2282(8)**	**¼**
Ow(1)	4c	**0**	**-0.048(2)**	**¼**

Figure S3. Representation of $FeF_{2.66}(OH)_{0.34}\cdot nH_2O$ in the two structural models (Orthorhombique *Cmcm* and Hexagonal P$6_3/m$)

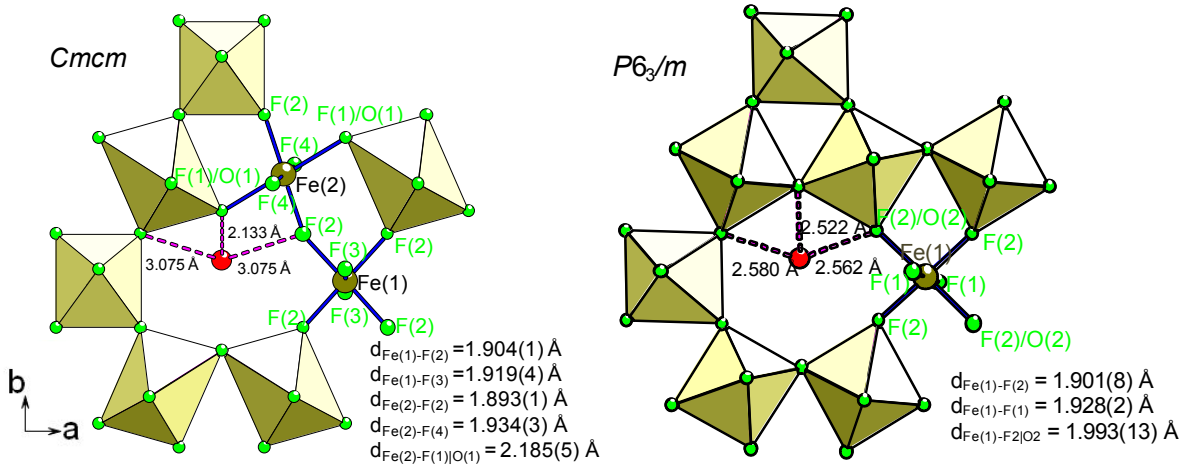

Figure S4. Refinements of the PDF data of the HTB phase using either $P6_3/m$ or *Cmcm* space group.

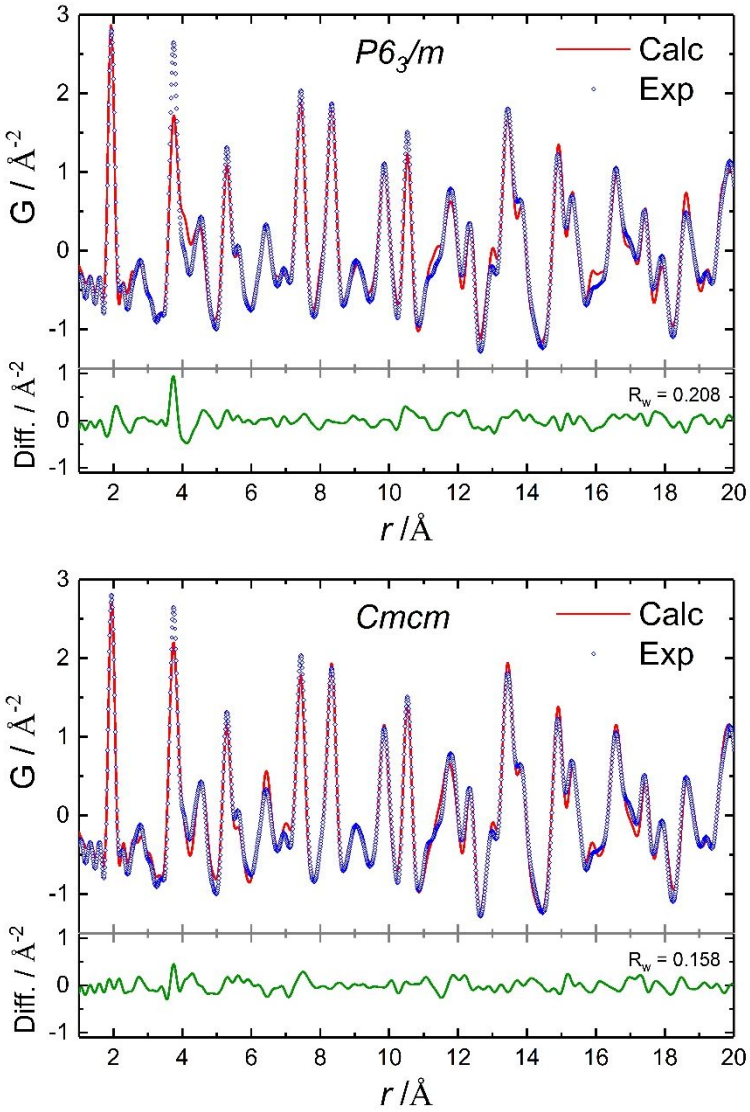

Figure S5. Voltage-composition profile of pyr-$FeF_{2.5}(OH)_{0.5}$ and HTB-$FeF_{2.66}(OH)_{0.34}$ in-situ XRD

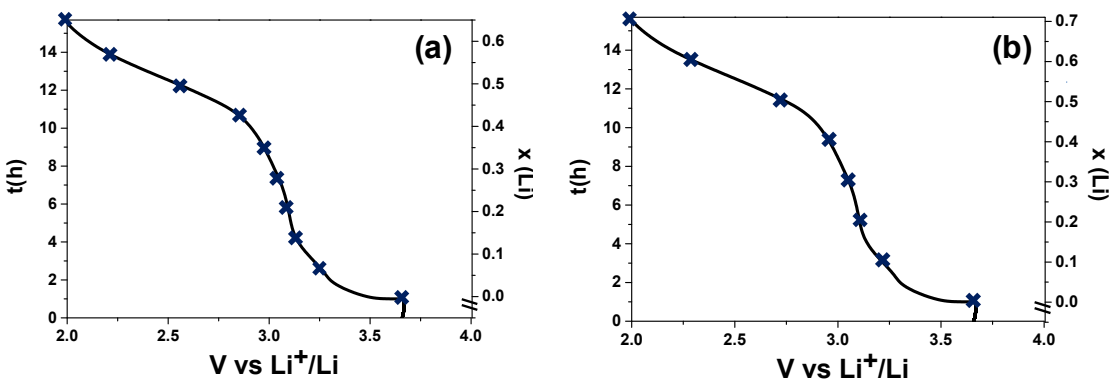

REFERENCES

1. Calage, Y.; Zemirli, M.; Greneche, J. M.; Varret, F.; De Pape, R.; Ferey, G., Mössbauer study of the new pyrochlore form of FeF_3. *J. Solid State Chem.* **1987,** *69* (2), 197-201.

2. Calage, Y.; Leblanc, M.; Ferey, G.; Varret, F., Mössbauer investigation of hexagonal tungsten bronze type FeIII fluorides: $(H_2O)_{0.33}FeF_3$ and anhydrous FeF_3. *J. Magn. Magn. Mater.* **1984,** *43* (2), 195-203.

3. Leblanc, M.; Ferey, G.; Chevallier, P.; Calage, Y.; De Pape, R., Hexagonal tungsten bronze-type Fe^{III} fluoride: $(H_2O)_{0.33}FeF_3$; crystal structure, magnetic properties, dehydration to a new form of iron trifluoride. *J. Solid State Chem.* **1983,** *47* (1), 53-58.

4. Guo, Y.; Gaczyński, P.; Becker, K. D.; Kemnitz, E., Sol–Gel Synthesis and Characterisation of Nanoscopic FeF_3-MgF_2 Heterogeneous Catalysts with Bi-Acidic Properties. *ChemCatChem* **2013,** *5* (8), 2223-2232.

5. Louvain, N.; Fakhry, A.; Bonnet, P.; El-Ghozzi, M.; Guérin, K.; Sougrati, M.-T.; Jumas, J.-C.; Willmann, P., One-shot versus stepwise gas–solid synthesis of iron trifluoride: investigation of pure molecular F_2 fluorination of chloride precursors. *CrystEngComm* **2013,** *15* (18), 3664-3671.

6. Duttine, M.; Dambournet, D.; Penin, N.; Carlier, D.; Bourgeois, L.; Wattiaux, A.; Chapman, K. W.; Chupas, P. J.; Groult, H.; Durand, E.; Demourgues, A., Tailoring the Composition of a Mixed Anion Iron-Based Fluoride Compound: Evidence for Anionic Vacancy and Electrochemical Performance in Lithium Cells. *Chem. Mater.* **2014,** *26* (14), 4190-4199.

7. Pohl, A.; Faraz, M.; Schröder, A.; Baunach, M.; Schabel, W.; Guda, A.; Shapovalov, V.; Soldatov, A.; Chakravadhanula, V. S. K.; Kübel, C.; Witte, R.; Hahn, H.; Diemant, T.; Behm, R. J.; Emerich, H.; Fichtner, M., Development of a water based process for stable conversion cathodes on the basis of FeF_3. *J. Power Sources* **2016,** *313*, 213-222.